Electronic Supplementary Information (ESI) for Chemical Communications

Strain-engineered upconversion nanoparticles for power-tunable dynamic information encryption

Changwen Li,[a] Yuqi Yang,[b] Jiaxiang Xiao,[a] Maijidan Nizhamu,[a] Shen Wang,[a] Qian Dong,[*a] Zhuo Chen[*a,b]

[a] *Molecular Science and Biomedicine Laboratory (MBL), State Key Laboratory of Chemo/Biosensing and Chemometrics, College of Chemistry and Chemical Engineering, College of Biology, Aptamer Engineering Center of Hunan Province, Hunan University, Changsha 410082, People's Republic of China*

[b] *College of Environmental Science & Engineering, Hunan University, Changsha 410082, People's Republic of China*

目录

1. Experimental

1.1. Materials and Reagents.

Unless otherwise specified, all chemical reagents were directly purchased from the merchants and used without further purification. Yttrium acetate tetrahydrate ($(CH_3COO)_3Y{\cdot}4H_2O$), Ytterbium acetate tetrahydrate ($(CH_3COO)_3Yb{\cdot}4H_2O$), Erbium acetate tetrahydrate ($(CH_3COO)_3Er{\cdot}4H_2O$), oleic acid (OA), etc. were purchased from Sigma Aldrich (St. Louis, MO, USA). Ammonium fluoride (NH_4F), cyclohexane, 1-octadecene(1-ODE), hexadecane, etc. were purchased from Merck Life Science Technology Co., Ltd. (Shanghai). Polystyrene (PS) microspheres were purchased from Jiangsu Zhichuan Technology. In the experiment, Oleylamine, Sodium Hydroxide (NaOH), methanol, ethanol, etc. were all purchased from Shanghai Titan Technology Co., Ltd.

1.2. Equipment.

The lattice structures of all the synthesized nanomaterials were obtained by the Bruker D8 Advance Polycrystalline X-ray diffractometer (XRD) at an angle range of 10-80°. The specific structures and morphologies of the synthesized nanoparticles were obtained by the JEM-2100 transmission electron microscope (TEM). The relevant energy dispersive spectra and high-resolution electron microscope imaging were obtained through the field emission transmission electron microscope (JEM-F200). The upconversion emission spectra were collected by the Hitachi F7100 fluorescence spectrometer with the excitation of an external 980 nm laser (Jilin Changchun New Industry Optoelectronics) in both continuous wave mode and pulse wave mode. The photoluminescence decay curve was measured by the steady state transient spectrometer (FLS980, Edinburgh Instruments Ltd), and the quantum yield was obtained by the steady state transient spectrometer (FLS1000, Edinburgh Instruments Ltd) under the excitation of the 980 nm laser. The absorption spectrum was obtained by the UV-Vis-NIR spectrophotometer (UV-2600i, Shimadzu Corporation).

1.3. Core-shell upconversion nanocrystal synthesis.

Core UCNPs with varying Yb^{3+} doping ratios (20%, 40%, 60%) were synthesized via a modified thermal decomposition method. In a typical procedure for the 20% Yb^{3+} sample, erbium, ytterbium, and yttrium acetate hydrates (molar ratio Er:Yb:Y = 2:20:78) were combined with 6 mL oleic acid (OA) and 15 mL 1-octadecene (1-ODE) in a 100 mL three-neck flask. The mixture was heated to 110°C under vigorous stirring for 30 min, then degassed and purged with N_2. Subsequently, the temperature was raised to 150°C and maintained for 30 min to form rare earth oleate complexes. After cooling to 50°C, 10 mL methanol solution containing NH_4F (4 mmol) and NaOH (2.5 mmol) was injected. The reaction mixture was stirred at 50°C for 30 min under N_2 atmosphere, then heated to 110°C to evaporate methanol. The solution was further degassed before being heated to 300°C at a rate of 20°min^{-1} and maintained for 1 h for nanocrystal growth. The resulting nanoparticles were purified by centrifugation (6000 rpm, 5 min) and washed twice with cyclohexane/ethanol (1:1, v/v). The final product was dispersed in 4 mL cyclohexane and stored at 4°C for further use.

Core-shell structures were prepared through epitaxial shell growth. Yttrium acetate hydrate (0.65 mmol) was dissolved in 6 mL OA and 15 mL 1-ODE in a 100 mL three-neck flask. After degassing at 110°C for 30 min and forming complexes at 150°C for 30 min under N_2, the solution was cooled to 50°C. The presynthesized core solution (in cyclohexane) was added, followed by dropwise addition of methanolic NH_4F (4 mmol) and NaOH (2.5 mmol). The subsequent reaction conditions and purification steps were identical to the core synthesis procedure.

$NaYF_4$:Yb@$NaYF_4$ particles were synthesized following the same protocol without Er^{3+} doping.

1.4. The measurement of absolute quantum yield (AQY)

The UCNPs were dispersed in cyclohexane to obtain a concentration of 20 mg/mL to ensure a relatively sufficient absorption (3-6%) of laser excitation light for accurate UCQYs measurement.[1] AQY measurements were conducted using the steady state transient spectrometer equipped with an integrating sphere. A continuous-wave 980 nm laser was employed as the excitation source. The excitation power density was

calibrated to 30 W/cm^2 at the sample position by adjusting the laser output and spot size. The measurement followed a two-step procedure. First, a blank quartz cuvette containing pure solvent was measured to obtain the total incident photon flux (L_{ref}) and background signal (E_{ref}). And then, the 20 mg/mL UCNPs dispersion were measured under identical conditions to determine the unabsorbed excitation photons (L_{sam}) and the emitted photons (E_{sam}). The AQY value was then calculated using Equation (S1).

$$AQY = \frac{E_{sam} - E_{ref}}{L_{ref} - L_{sam}} \times 100\% \quad \text{(S1)}$$

1.5. UCNPs inks.

The UCNPs inks (20 mg mL^{-1}) were formulated by mixing a concentrated UCNP cyclohexane dispersion (34 mg mL^{-1}, 60 vol%) with hexadecane (35 vol%) to elevate the boiling point, oleylamine (3 vol%) to reduce surface tension, and polystyrene microspheres (2 vol%) as a viscosity modifier. This specific composition was critical for balancing fluid dynamics during the patterning process. And following treatment with 0.2 M HCl, the UCNPs were rendered hydrophilic. The UCNPs inks were subsequently formulated by mixing the aqueous UCNPs dispersion (34 mg mL^{-1}, 70 vol%) with glycerol (25 vol%) and an aqueous PVP solution (5 wt%, 5 vol%).

1.6. Multi-pattern Imaging by UCNPs

The UCNPs inks were hand-written onto standard A4 paper using a glass capillary tube to form the specific patterns. And the patterns were irradiated using a power-tunable 980 nm LED with a collimated spot diameter of approximately 2 cm. Sequential pattern display was achieved by continuously increasing the excitation power, and the resulting luminescence was recorded using a smartphone with a specific band-pass filter (NBP520-40K) to strictly rule out interference from the 980 nm excitation scatter during image acquisition. This filter possesses a center wavelength of 520 nm with a full width at half maximum (FWHM) of 40 nm. It is designed to selectively transmit the characteristic green emission of the Er^{3+} ions while providing high optical density blocking the 980 nm light.

Supporting Figures

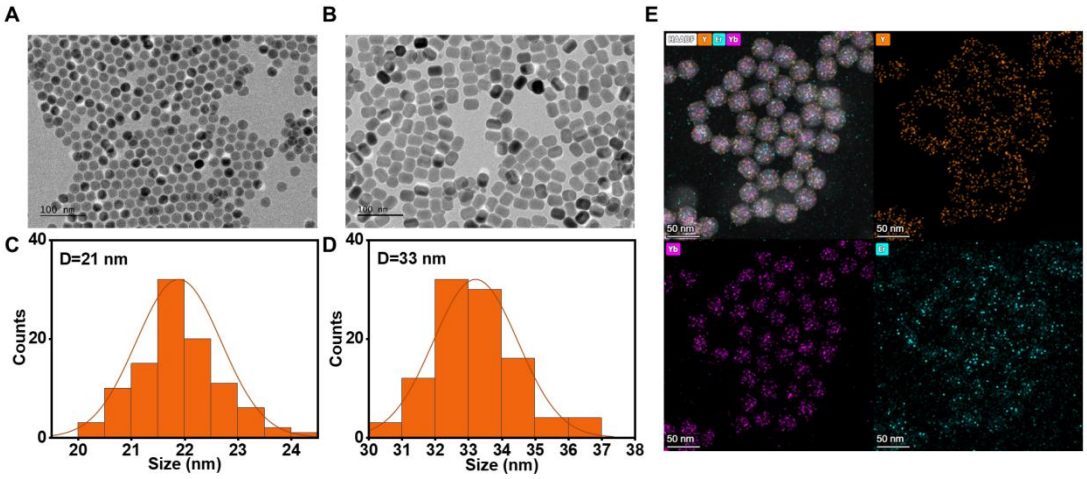

Fig. S1 Fabrication of core-shell structured UCNPs. The TEM images of (A) $NaYF_4$:Yb,Er core nanoparticles and (B) $NaYF_4$:Yb,Er@$NaYF_4$ core-shell nanoparticles. The size histograms of (C) $NaYF_4$:Yb,Er core nanoparticles and (D) $NaYF_4$:Yb,Er@$NaYF_4$ core-shell nanoparticles. (E) The EDS elemental mapping image of core-shell UCNPs.

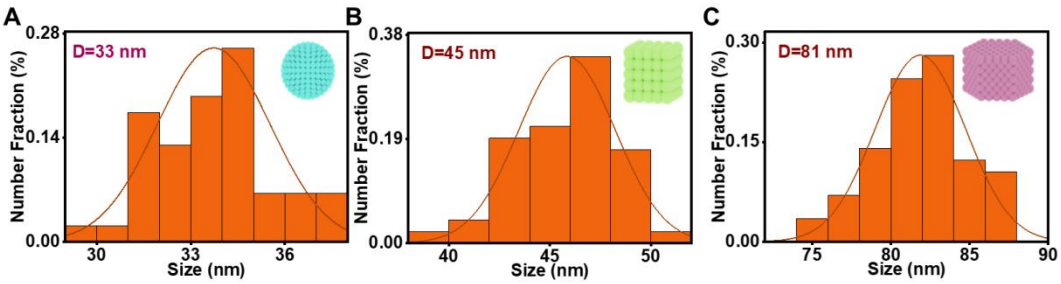

Fig. S2 The size histograms of UCNPs. (A) $NaYF_4$:20%Yb,2%Er@$NaYF_4$, (B) $NaYF_4$:40%Yb,2%Er@$NaYF_4$ and (C) $NaYF_4$:60%Yb,2%Er@$NaYF_4$.

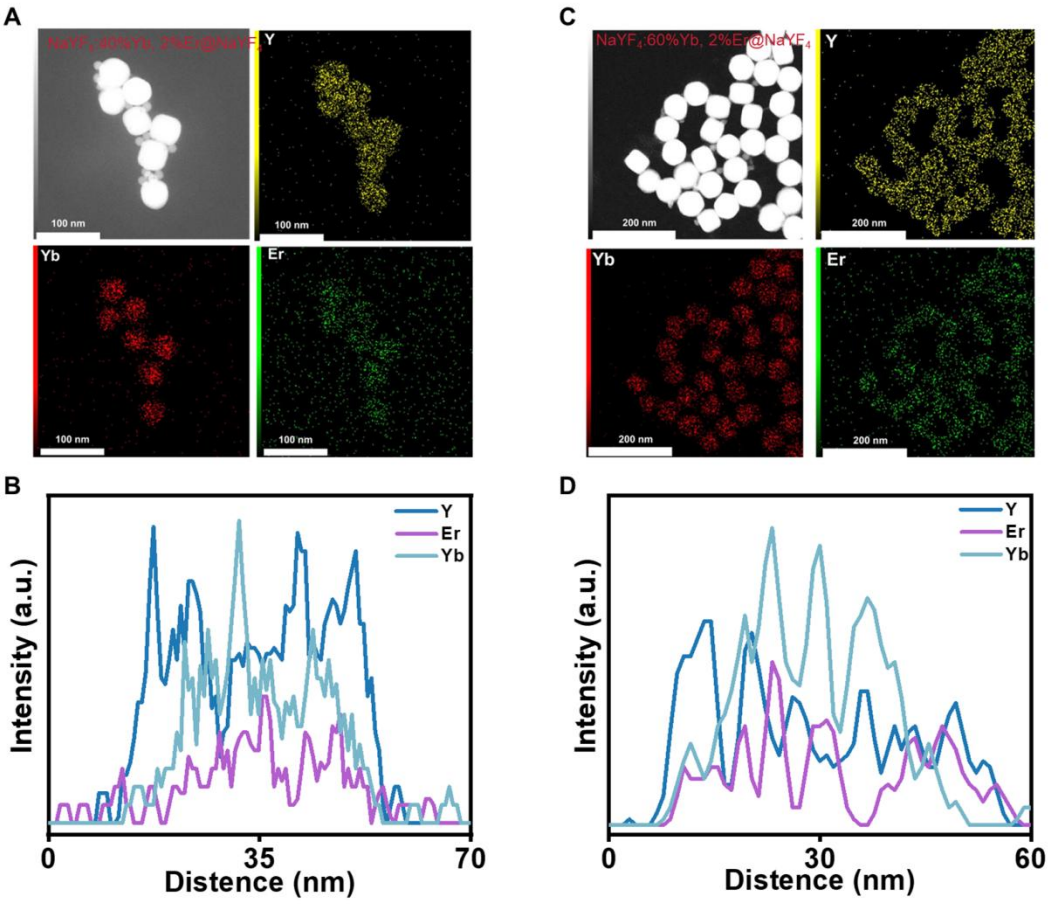

Fig. S3 The EDS elemental mapping images of (A) $NaYF_4$:40%Yb, 2%Er@$NaYF_4$ and (C) $NaYF_4$:60%Yb, 2%Er@$NaYF_4$. (B, D) The EDS elemental line scan profile across a single particle corresponding to A and C.

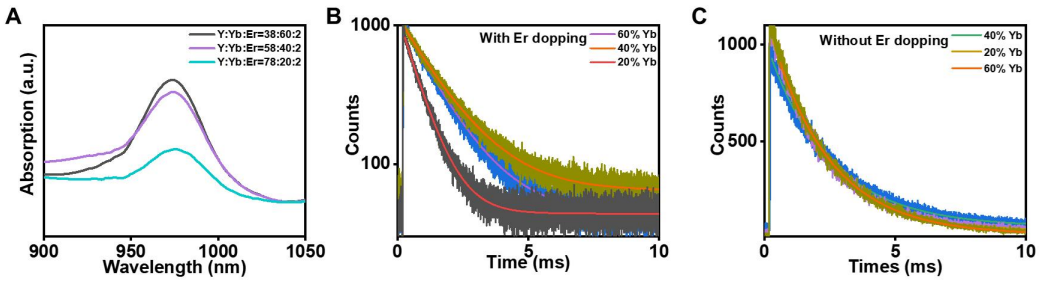

Fig. S4 The mechanism of energy migration process in UCL. (A) Near-infrared absorption spectrum of different UCNPs at 980 nm. (C) The luminescence lifetimes of Yb without Er doped and (D) with Er dopped, excititation 975 nm, emmission 1030 nm.

It can be seen from Fig. S4B that the luminescence lifetime of Yb does not vary much regardless of the doping concentration. However, when Er is added, there is a difference. When the doping concentration of Yb^{3+} is 40%, the luminescence lifetime increases compared to 20%. We attribute this to the cross relaxation caused by the energy transfer between Er^{3+} and Yb^{3+}, thereby reducing the energy migration efficiency.

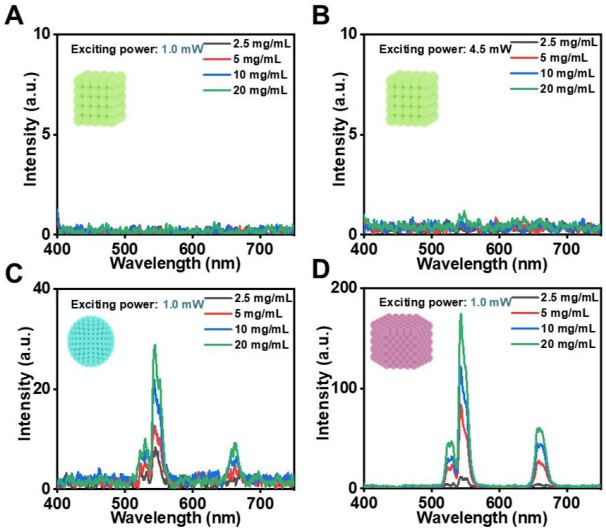

Fig. S5 The relationship between signals and concentrations at UCL. The UC emission spectra of (A, B) $NaYF_4$:40%Yb, 2%Er@$NaYF_4$, (C) $NaYF_4$:60%Yb, 2%Er@$NaYF_4$ and (D) $NaYF_4$:20%Yb, 2%Er@$NaYF_4$ with different excitation powers.

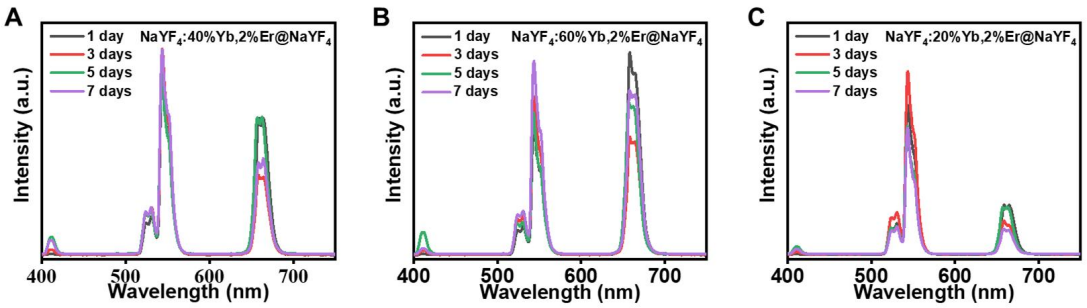

Fig. S6 Characterization of long-term stability of the developed UCNPs. (A) The UCL spectrum of $NaYF_4$:40%Yb,2%Er@$NaYF_4$ recorded after being stored for 1, 3, 5, and 7 days under ambient conditions. (B) The UCL spectrum of $NaYF_4$:60%Yb,2%Er@$NaYF_4$ recorded after being stored for 1, 3, 5, and 7 days under ambient conditions. (C) The UCL spectrum of $NaYF_4$:20%Yb,2%Er@$NaYF_4$ recorded after being stored for 1, 3, 5, and 7 days under ambient conditions.

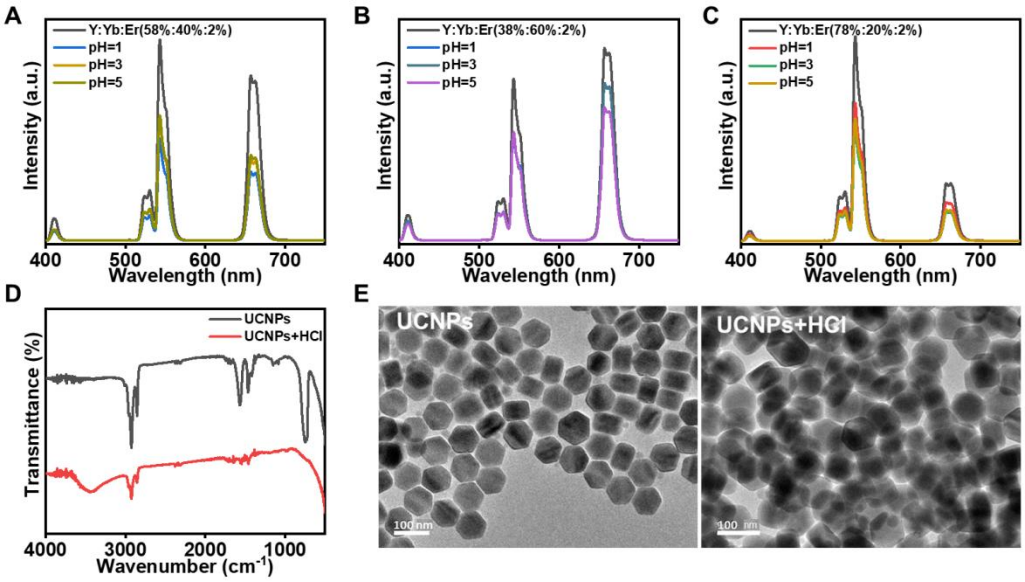

Fig. S7 Characterization of acid corrosion resistance of the developed UCNPs. (A) The UCL spectrum of the pristine UCNPs (Y:Yb:Er 58%:40%:2%) and after immersion in acidic solutions with varying pH values (pH=1, 3 and 5) for 1 h. (B) The UCL spectrum of the pristine UCNPs (Y:Yb:Er 38%:60%:2%) and after immersion in acidic solutions with varying pH values (pH=1, 3 and 5) for 1 h. (C) The UCL spectrum of the pristine UCNPs (Y:Yb:Er 78%:20%:2%) and after immersion in acidic solutions with varying pH values (pH=1, 3 and 5) for 1h. (D) The FTIR spectra of UCNPs with and without HCl treatment. The disappearance of C-H stretching bands (2800-3000 cm^{-1}) and the appearance of the O-H band (~3400 cm^{-1}) confirm the removal of oleic acid. (E) TEM images of UCNPs with and without HCl treatment. Scale bars: 100 nm.

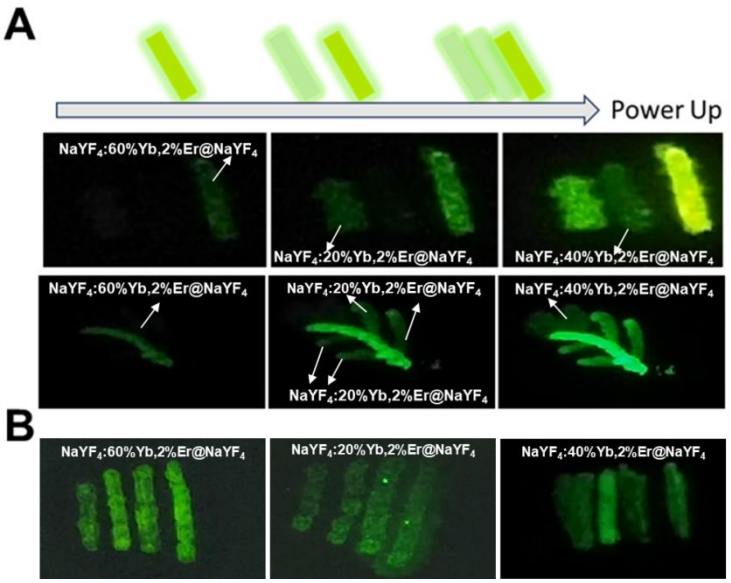

Fig. S8 Photos under different particle encodings with a 980 nm LED excitation. (A) Time diagram showing the appearance of different particle-encoded patterns as power increases. (B) UCL luminescence images of the same particle with different concentrations under varying power conditions, the concentrations in the figure decreased from left to right. The concentration of all the nanoparticles used for writing is 20 mg/mL.

It can be seen from Fig. S6A that different particles exhibit different patterns of signal appearance as the power increases. The Fig. S6B shown this signal response was shown to be independent of the particle concentration.

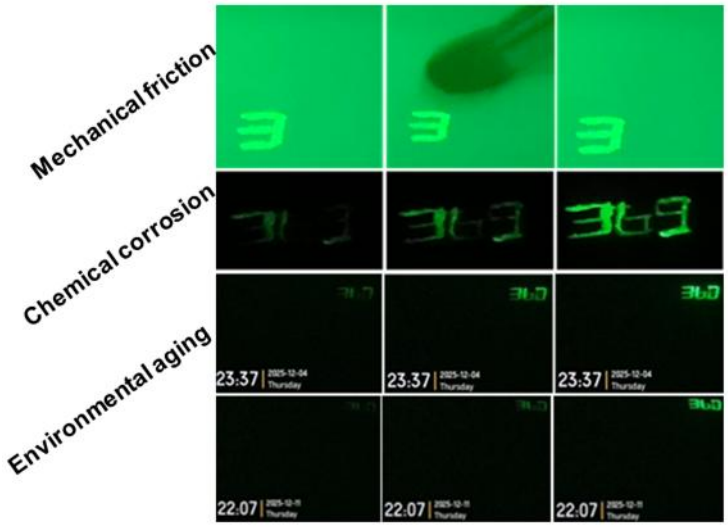

Fig. S9 Photographs of UCNPs printed patterns under 980 nm excitation subjected to mechanical friction, chemical corrosion tests, and continuous environmental aging, confirming their robustness for real-world applications.

Table S1. The corresponding element contents of UCNPs.

Sample	Element	amount of substance(mmol)[1]
$NaYF_4$:20% Yb,2% Er@$NaYF_4$	Yb	0.53
	Er	0.05
$NaYF_4$:40% Yb,2% Er@$NaYF_4$	Yb	0.55
	Er	0.026
$NaYF_4$:60% Yb,2% Er@$NaYF_4$	Yb	0.56
	Er	0.016

[1] The percent value is the average of two parallel experiments.

References

1. C. M. Jones, A. Gakamsky, J.Marques-Hueso, *Science and Technology of Advanced Materials*, **2021**, *22*(1), 810-848.